Eur Spine J (2009) 18:1971–1977
DOI 10.1007/s00586-009-1140-4

ORIGINAL ARTICLE

Influence of asymmetric tether on the macroscopic permeability of the vertebral end plate

Jean Michel Laffosse · Franck Accadbled · Thierry Odent · Thibault Cachon · Anne Gomez-Brouchet · Dominique Ambard · Eric Viguier · Jérôme Sales de Gauzy · Pascal Swider

Received: 15 December 2008 / Revised: 29 July 2009 / Accepted: 9 August 2009 / Published online: 20 August 2009

Abstract We implemented an experimental model of asymmetrical compression loading of the vertebral end plate (VEP) in vivo. The macroscopic permeability of the VEP was measured. We hypothesized that static asymmetrical loading on vertebrae altered the macroscopic permeability of the VEP. In scoliosis, solute transport to and from the disc is dramatically decreased especially at the apical intervertebral disc. The decrease in permeability could be induced by mechanical stress. Nine skeletally immature pigs were instrumented with left pedicle screws and compression rod at the T5/T6 and L1/L2 levels. After 3 months, three cylindrical specimens of the VEP were obtained from each of the tethered levels. A previously validated method for measuring permeability, based on the relaxation pressure due to a transient-flow rate was used. A pistoning device generated a fluid flow that fully saturated the cylindrical specimen. The decrease in upstream pressure was measured using a pressure transducer, which allowed the macroscopic permeability to be derived. A microscopic study completed the approach. Overall macroscopic permeability was lower for the tethered VEPs than for the VEPs of the control group, respectively −47% for flow-in ($p = 0.0001$) and −46% for flow-out ($p = 0.0001$). In the tethered group, macroscopic permeability of the specimens from the tethered side was lower than macroscopic permeability of those from the non-tethered side, −39% for flow-out ($p = 0.024$) and −47% for flow-in ($p = 0.13$). In the control group, the macroscopic permeability was greater in the center of the VEP than in its lateral parts for flow-out ($p = 0.004$). Macroscopic permeability of the center of the VEPs was greater for flow-out than for flow-in ($p = 0.02$). There was no significant difference between thoracic and lumbar. This study demonstrated that compression loading applied to a

Electronic supplementary material The online version of this article (doi:10.1007/s00586-009-1140-4) contains supplementary material, which is available to authorized users.

J. M. Laffosse
Department of Orthopaedic Surgery, Toulouse Rangueil University Hospital, Toulouse, France

J. M. Laffosse · F. Accadbled · D. Ambard · J. Sales de Gauzy · P. Swider
Biomechanics Laboratory, Toulouse University Hospital, Toulouse, France

F. Accadbled · J. Sales de Gauzy
Department of Paediatric Orthopaedic Surgery, Hôpital des Enfants, Toulouse, France

T. Odent
Department of Orthopaedic Surgery, Hôpital des Enfants Malades, Assistance-Publique Hôpitaux de Paris, Université Paris V René Descartes, Paris, France

T. Odent · T. Cachon · E. Viguier
Department of Surgery, National Veterinary School, Lyon, France

A. Gomez-Brouchet
Department of Pathology, Toulouse Rangueil University Hospital, Toulouse, France

F. Accadbled (✉)
Service de Chirurgie Orthopédique et Traumatologique, Hôpital des Enfants, 330, avenue de Grande Bretagne, 31059 Toulouse Cedex 9, France
e-mail: faccadbled@wanadoo.fr

growing spine results in decreased permeability of the VEP. This result could be explained by local remodeling, such as calcification of the cartilage end plate or sclerosis of the underlying bone.

Keywords Vertebral endplate · Permeability · Experimental method · Growth · Animal model

Introduction

Biomechanical properties of the intervertebral disc (IVD) rely on its hydration, tissue organization and the composition of its extracellular matrix [8, 15, 24]. Even though it is avascular and has low cell content, the IVD has a metabolism. Solutes exchange occurs through the matrix of the annulus fibrosus (AF) and the nucleus pulposus (NP) via passive diffusion and active convection [11–13, 28]. Convection is based upon fluid exchange which occurs mostly through the vertebral end plate (VEP) [6, 20, 22]. This nutrition route is precarious [22, 30]. It may be compromised in case of VEP degeneration [1, 9] but also in scoliosis [30]. The composition of the IVD is then altered and it eventually degenerates [2, 4, 7, 10, 32]. Several studies investigated the influence of an experimental scoliosis on the VEP and IVD composition [5, 17, 27]. Nachemson [16] was the first to correlate the permeability of the VEP with IVD degeneration. Nevertheless there has been virtually no direct measurement of macroscopic permeability of the pathologic VEP because no suitable method has been available.

We hypothesized that static asymmetrical mechanical loading of the vertebrae altered the macroscopic permeability of the VEP. To proceed, we implemented our study in a porcine animal model.

Materials and methods

Specimen preparation

Nine 4-week-old skeletally immature pigs were instrumented with 2 left pedicle screws connected together in situ via a titanium rod at T5/T6 and L1/L2 levels (Ø 4 mm, 28 mm titanium screws, Medtronic®, Minneapolis, USA). After 3 months, the animals were killed and their thoracic and lumbar spine harvested 'en bloc' and then immersed into normal saline added with heparin (100 IU/ml). To prevent formation of blood clots, we injected low molecular weight heparin (Innohep® Tinzaparin, Leo Pharma Inc.), 4,500 IU/ml once a day for 2 days before harvest. All experiments were carried out in accordance with the animal welfare regulations and guidelines. Anteroposterior, lateral radiographs and CT scan of those instrumented spines were undertaken (Fig. 1). The VEPs adjacent to the T5–T6 and L1–L2 IVD were separated using a powered saw blade along with 2 VEPs harvested 3 levels above the thoracic tether and below the lumbar tether. The latter were free from any previous dissection or deformity and represented the control group. The IVD was removed from each plate using a beaver blade under binocular microscope. Great care was taken to avoid any injury to the cartilage end plate (CEP). Then, 3 cylindrical specimens of 5-mm diameter and 6-mm length each were harvested from each VEP using a custom-made stainless steel cylindrical punch. Each specimen comprised 4 layers: CEP,

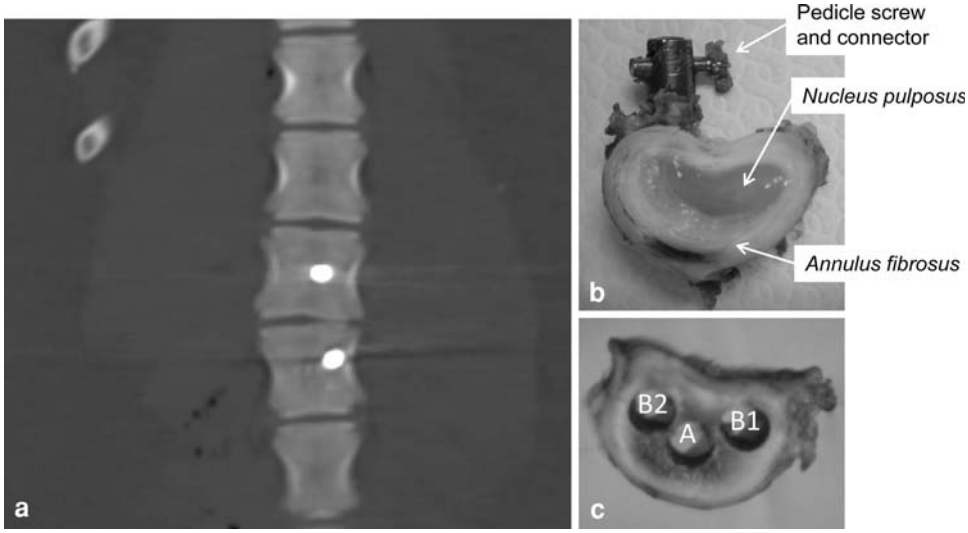

Fig. 1 Lumbar spine instrumented with left posterior tether. **a** CT scan, coronal view showing L1 and L2 left pedicle screws and L1–L2 disc wedging; **b** Inferior vertebral end plate of L1 with left pedicle screw; **c** Inferior vertebral end plate of L1 after disc excision and specimens harvest. B2 sample was harvested on the instrumented side of the vertebra

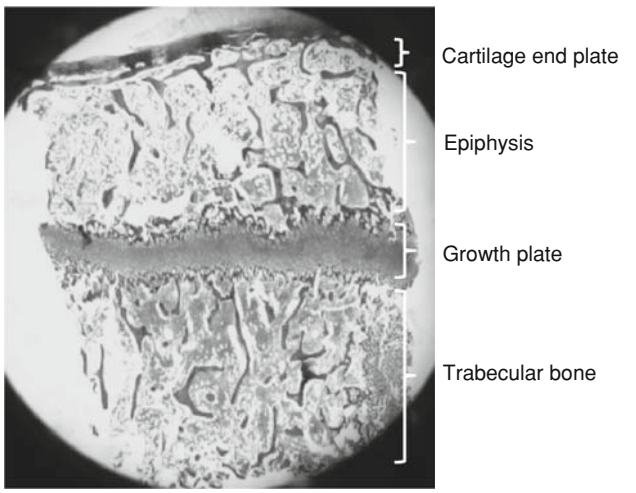

Fig. 2 Microscopic section of a plug as harvested from the vertebral end plate, original magnification, ×1

epiphysis, growth plate and adjacent trabecular bone (Fig. 2). One specimen was taken from the central zone (A) and 2 were taken laterally, right (B1) and left (B2). The edge of the specimen was at least 1.5-mm away from a screw. The specimens were carefully inserted into silicone tubes and then frozen for storage within 6 h at −23°C in Ringer's solution added with 10% cryoprotectant Dimethyl sulfoxide (DMSO) and 100 IU/ml heparin. The specimens were gradually defrosted later on. All the specimens were studied in microscopy after the permeability measurement and the trabecular bone checked for any necrosis or sclerosis. No such damage was noticed (Fig. 3).

Testing apparatus and protocol

A previously validated method for measuring permeability, based on the relaxation pressure due to a transient-flow rate was used [1]. The specimens were placed in the testing apparatus and a pistoning device generated a fluid flow that fully saturated the cylindrical specimen with a maximal pressure of 0.1 to 0.2 MPa. The decrease of upstream pressure $P(t)$ was measured using a pressure transducer (TME®, 0–5 bars) and Labview® software (National Instrument), which allowed the macroscopic permeability κ/μ to be derived using Eq. 1. Parameters P_0, μ, β, respectively were the initial pressure, the fluid viscosity and the coefficient of the fixture previously calibrated.

$$P(t) = P_0\, e^{\left[\left(\frac{\kappa}{\mu}\right)\Big/\beta\right]t} \qquad (1)$$

Three measurements were achieved for each specimen and fluid direction (flow-in and flow-out of the IVD); the 3

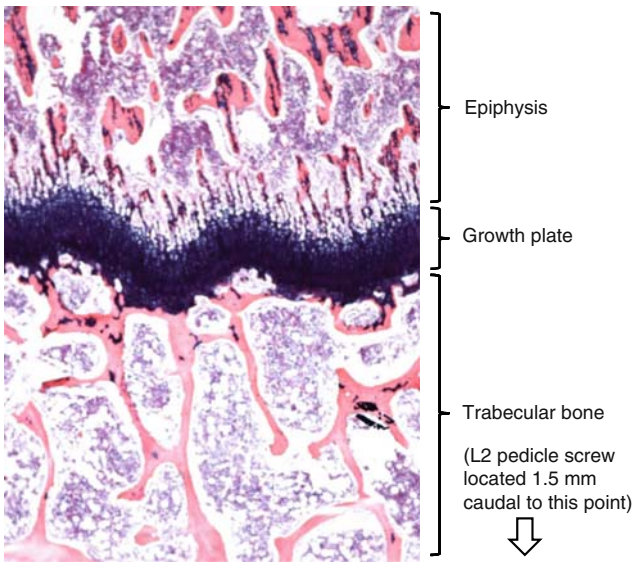

Fig. 3 Microscopic section of B2 plug as harvested from the cranial vertebral end plate of instrumented L2. No bone reaction in relation with the vicinity of the screw. Original magnification, ×4

values were then averaged for each flow direction. Each specimen was then fixed in formalin and stored for later microscopic study.

Microscopic study

Specimens were embedded in paraffin and cut in half longitudinally. The thickness of each of the following layers (CEP, epiphysis and growth plate) was measured on six different spots and averaged.

Statistical analysis

Means are presented in 10^{-14} m^4/Ns with standard deviation (SD). Variances were compared using Levene's test. Shapiro-Wilk test assessed normality of distributions. Student's t test was used for mean comparisons in case of normal distributions of continuous variables. Otherwise, the Wilcoxon and Kruskal–Wallis non-parametric tests were chosen. The level of statistical significance was $p = 0.05$. Data were analyzed using Statview® statistical software (SAS Institute Inc., USA).

Results

Permeability

Variation with loading

Overall macroscopic permeability was lower for the tethered VEPs than for the VEPs of the control group,

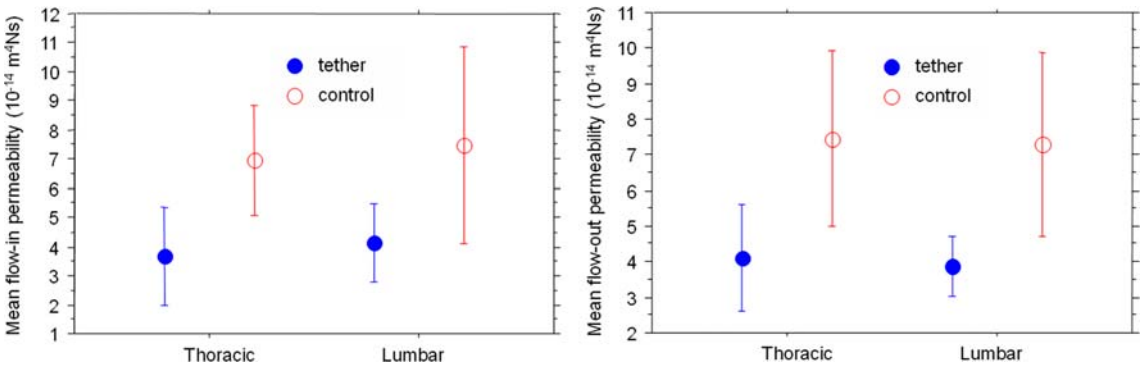

Fig. 4 Mean macroscopic permeability for tethered (*solid ring*) and control (*empty ring*) groups. **a** flow in; **b** flow out

respectively, 3.82 [SD 5.57] vs. 7.2 [SD 9.49] for flow-in (−47%, $p = 0.0001$) and 3.98 [SD 4.35] vs. 7.37 [SD 8.70] for flow-out (−46%, $p = 0.0001$) (Fig. 4).

In the tethered group, macroscopic permeability of B2 specimens (tethered side) was lower than macroscopic permeability of B1 specimens, both for flow-in 2.65 [SD 2.77] vs. 5.02 [SD 8.42] (−47%, $p = 0.13$) and flow-out 2.59 [SD 2.35] vs. 4.22 [SD 4.52] (−39%, $p = 0.024$).

Kruskal–Wallis test demonstrated that values of permeability for specimens A, B1 and B2 were significantly different both for flow-in ($p = 0.03$) and flow-out ($p = 0.002$).

Variations with location

In the control group, the macroscopic permeability was greater in the center of the VEP 9.45 [SD 10.83] than in its lateral parts 6.41 [SD 7.41] for flow-out ($p = 0.004$). This difference was not significant for flow-in ($p = 0.09$).

Variations with flow direction

Macroscopic permeability of the center of the VEPs of both groups was greater for flow-out 5.18 [SD 5.36] than for flow-in 4.09 [SD 3.57] ($p = 0.02$).

There was no significant difference between thoracic and lumbar VEPs neither in the tethered group nor in the control group ($p = 0.18$). The permeability values for thoracic and lumbar VEPs are displayed in Tables 1 and 2, respectively.

Microscopic study

Tethered VEPs

CEP was thinner in A than in B2 ($p = 0.01$). There was no significant difference of thickness between A and B1 ($p = 0.14$) and between B1 and B2 ($p = 0.15$). Epiphysis was thinner in A than in B1 ($p < 0.0001$) and in B2 ($p < 0.0001$). There was no significant difference between B1 and B2 ($p = 0.61$). The growth plate was thinner in A than in B1 ($p = 0.01$) and B2 ($p = 0.002$). There was no significant difference between B1 and B2 ($p = 0.84$).

Control group

CEP was thinner in A than in B1 (right lateral specimen) and in B2 (left lateral specimen) but the difference was not significant ($p = 0.06$ and 0.08, respectively). There was no significant difference of thickness between B1 and B2 ($p = 0.78$). Epiphysis was thinner in A than in B1 ($p = 0.0007$) and in B2 ($p < 0.0001$). There was no significant difference between B1 and B2 ($p = 0.28$). The growth plate was thinner in A than in B1 ($p = 0.03$) and B2 ($p = 0.01$). There was no significant difference between B1 and B2 ($p = 0.33$).

Tethered VEPs versus control group

There was no significant difference of thickness for all 3 layers (CEP, subchondral bone and growth plate) in all 3

Table 1 Mean macroscopic permeability of the thoracic VEPs

	Control			Tethered			
	Central	Lateral	Mean	Central	B1	B2	Mean
Flow in	7.11 (6.21)	6.88 (6.79)	6.95 (6.55)	3.34 (2.23)	5.48 (10.03)	2.16 (2.04)	3.69 (6.14)
Flow out	8.10 (8.97)	7.15 (8.49)	7.44 (8.55)	5.25 (6.89)	4.61 (5.69)	2.32 (2.21)	4.10 (5.40)

Values are in 10^{-14} m^4/Ns with standard deviation (SD)

Table 2 Mean macroscopic permeability of the lumbar VEPs

	Control			Tethered			
	Central	Lateral	Mean	Central	B1	B2	Mean
Flow in	12.12 (19.27)	5.19 (4.26)	7.45 (11.79)	4.85 (4.48)	4.57 (6.8)	3.07 (3.27)	4.13 (5.02)
Flow out	8.1 (8.97)	7.15 (8.49)	7.3 (8.92)	3.42 (3.42)	3.84 (3.14)	2.94 (2.94)	3.88 (3.12)

Values are in 10^{-14} m^4/Ns with standard deviation (SD)

locations (A, B1 and B2) between the index and control groups.

Discussion

We implemented an experimental model of asymmetrical compression loading of the VEP. Compression was the result of restrained longitudinal growth on the tethered vertebrae. The current results confirmed that the permeability is greater in the center than in the periphery of the VEP in relation with a lower thickness of its constitutive layers [1]. It also confirmed the influence of fluid flow direction, macroscopic permeability being greater for flow-out than flow-in [1]. Finally, compression loading affected the macroscopic permeability of the VEP that was lower in the tethered group than in the control group. We were not able to correlate the lower permeability of the tethered VEPs with the microscopic findings.

According to the Hueter Volkmann principle, an angular deformity that is asymmetrically loaded is likely to progress. Roaf hypothesized in 1960 that a 'vicious circle' develops in the progression of scoliosis, assuming that the growth is inhibited in the concave side and unrestrained on the convex side [18]. This has been confirmed since then by experimental studies [25, 26]. Asymmetrical loading has also a significant influence at the level of the VEP–IVD interface [5, 17, 27] with remodeling of the VEP and calcifications of the CEP resulting in decreased permeability and eventually disc degeneration [16, 19, 21, 29, 30]. This cascade can be represented as another 'vicious circle' which affects the permeability of the VEP (Fig. 5). Several studies demonstrated the strong interaction between spine curvature, IVD composition and permeability of the VEP. Taylor et al. [27] performed in 1976 a posterior lumbar tether on skeletally immature dogs. After 3 months, no difference was noted on histological examination as compared to the control group. However, it resulted after 6 months in experimental scoliosis and narrowing of the intervening IVD as well as decreased concentration in collagen of the NP. These findings suggest a temporary tolerance to the mechanical stress [23]. Newton et al. [17] carried out an anterolateral tethering of the spine in a growing ovine model by using a pretensioned cable. They

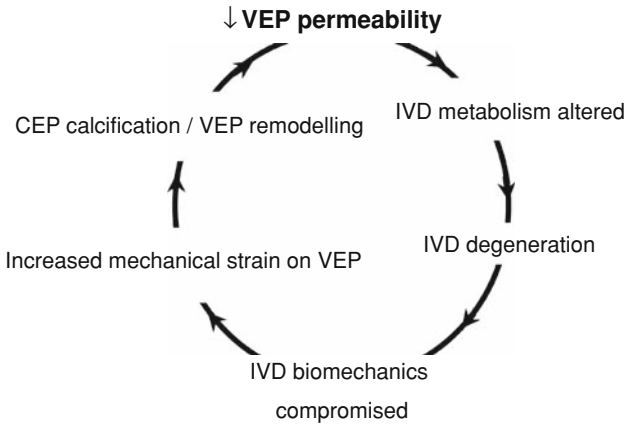

Fig. 5 The 'vicious circle' of the permeability

observed after 3 months a significant wedging of the IVD as well as lower height of the vertebral bodies on the tethered side. Braun et al. [23] created an experimental structural scoliosis in an immature goat model by using 2 sublaminar wires and a posterior rod from T5 to L1 along with convex rib resection and concave rib tethering. Initial scoliosis after asymmetrical tethering measured 42° on average and progressed significantly to 60° on average after 6 to 15 weeks, with substantial wedging of vertebrae and discs. Histology demonstrated concave trabecular and cortical thickening of the vertebral bodies and bone drift toward the concavity. Discs analysis showed fibrosis and disorganization of the concave AF, NP was displaced toward the convexity. After 15 weeks, IVD composition was also affected with general decrease of hydroxyprolin content and decrease of prostaglandin in the NP. Concentration in prostaglandin and hydroxyprolin were decreased in the concavity of the apical IVDs.

Other authors investigated the influence of scoliotic deformity on the permeability of the VEP in human, as measured indirectly from Nitrous oxide and then Oxygen diffusion to the IVD [3, 30]. Urban et al. [30] in 2001 found that relative permeability was severely reduced at the apical IVD of neuromuscular scoliosis. This was later confirmed by Bibby et al. [3] who found the apical IVD had the lowest oxygen and highest lactate concentrations and lowest total number of cells. Cell viability and glucose concentration were lower toward the convex side of the

curve. Even though it showed the influence of asymmetrical loading on the permeability of the VEP, this latter result differs from our above mentioned results. This could be explained by the fact that they investigated permeability in vivo in real scoliosis in human, whereas we measured macroscopic permeability in animals shortly after a single level tether, resulting in very different stresses upon the apical IVD.

These modifications at the level of the IVD could remain reversible to a certain extent if the spine is rebalanced and even loading is restored. Violas et al. [31] reported of MRI-based objective quantification of the volume and NP/AF ratio of lumbar IVDs below a posterior instrumentation for idiopathic scoliosis. IVD volume and NP/AF ratio were significantly increased after instrumentation as compared to preoperative values, highly suggesting IVD rehydration after proximal spine had been rebalanced and normal loading restored.

The main shortcomings of the current study are the direct surgical approach of the tethered levels which vascularization could therefore have been compromised. It could also have generated fibrous scar tissue. However, IVDs were carefully scrutinized for screw penetration. The compression load applied to the VEP was static, whereas a greater impact of dynamic loading on bone remodeling, such as in scoliosis as been suggested [14].

This study demonstrated that asymmetrical compression stress applied to a growing spine results in decreased permeability of the VEP. Therefore, hydration of the disc may be altered, leading subsequent degenerative changes. We currently implement coupled histological and micro CT studies to further investigate these complex mechanobiological phenomena.

Conflict of interest statement None.

References

1. Accadbled F, Ambard D, Sales de Gauzy J, Swider P (2008) A measurement technique to evaluate the macroscopic permeability of the vertebral end-plate. Med Eng Phys 30(1):116–122
2. Akhtar S, Davies J, Caterson B (2005) Ultrastructural localization and distribution of proteoglycan in normal and scoliotic lumbar disc. Spine 30(11):1303–1309
3. Bibby SR, Fairbank JC, Urban MR, Urban JP (2002) Cell viability in scoliotic discs in relation to disc deformity and nutrient levels. Spine 27(20):2220–2228 discussion 2227–2228
4. Bibby SR, Meir A, Fairbank JC, Urban JP (2002) Cell viability and the physical environment in the scoliotic intervertebral disc. Stud Health Technol Inform 91:419–421
5. Braun J, Ogilvie J, Akyuz E, Brodke D, Bachus K, Stefko R (2003) Experimental scoliosis in an immature goat model: a method that creates idiopathic-type deformity with minimal violation of the spinal elements along the curve. Spine 28(19):2198–2203
6. Brodin H (1955) Path of nutrition in articular cartilage and the intervertebral disk. Acta Orthop Scand 24:177–183
7. Chen B, Fellenberg J, Wang H, Carstens C, Richter W (2005) Occurrence and regional distribution of apoptosis in scoliotic discs. Spine 31(5):519–524
8. Costi JJ, Hearn TC, Fazzalari NL (2002) The effect of hydration on the stiffness of intervertebral discs in an ovine model. Clin Biomech (Bristol, Avon) 17(6):446–455
9. Donisch E, Trapp W (1971) The cartilage endplates of the human vertebral column (some considerations of postnatal development). Anat Rec 169:705–716
10. Duance V, Crean J, Sims T, Avery N, Smith S, Menage J, Eisenstein S, Roberts S (1998) Changes in collagen cross-linking in degenerative disc disease and scoliosis. Spine 23(23):2545–2551
11. Grunhagen T, Wilde G, Soukane D, Shirazi-Adl S, Urban J (2006) Nutrient supply and intervertebral disc metabolism. J Bone Joint Surg Am 88(Suppl 2):30–35
12. Holm S, Maroudas A, Urban JP, Selstam G, Nachemson A (1981) Nutrition of the intervertebral disc: solute transport and metabolism. Connect Tissue Res 8(2):101–119
13. Katz M, Hargens A, Garfin S (1986) Intervertebral disc nutrition. Diffusion versus convection. Clin Orthop 210:243–245
14. Lanyon LE, Rubin CT (1984) Static vs dynamic loads as an influence on bone remodelling. J Biomech 17(12):897–905
15. Maroudas A, Stockwell RA, Nachemson A, Urban J (1975) Factors involved in the nutrition of the human lumbar intervertebral disc: cellularity and diffusion of glucose in vitro. J Anat 120(1):113–130
16. Nachemson A, Lewin T, Maroudas A, Freeman MA (1970) In vitro diffusion of dye through the end-plates and the annulus fibrosus of human lumbar inter-vertebral discs. Acta Orthop Scand 41(6):589–607
17. Newton PO, Fricka KB, Lee SS, Farnsworth CL, Cox TG, Mahar AT (2002) Asymmetrical flexible tethering of spine growth in an immature bovine model. Spine 27(7):689–693
18. Roaf R (1960) Vertebral growth and its mechanical control. J Bone Joint Surg Br 42-B:40–59
19. Roberts S, Menage J, Eisenstein SM (1993) The cartilage endplate and intervertebral disc in scoliosis: calcification and other sequelae. J Orthop Res 11(5):747–757
20. Roberts S, Menage J, Urban JP (1989) Biochemical and structural properties of the cartilage end-plate and its relation to the intervertebral disc. Spine 14(2):166–174
21. Roberts S, Urban JP, Evans H, Eisenstein SM (1996) Transport properties of the human cartilage endplate in relation to its composition and calcification. Spine 21(4):415–420
22. Selard E, Shirazi-Adl A, Urban J (2003) Finite element study of nutrient diffusion in the human intervertebral disc. Spine 28(17):1945–1953
23. Setton LA, Chen J (2006) Mechanobiology of the intervertebral disc and relevance to disc degeneration. J Bone Joint Surg Am 88(Suppl 2):52–57
24. Setton LA, Zhu W, Weidenbaum M, Ratcliffe A, Mow VC (1993) Compressive properties of the cartilaginous end-plate of the baboon lumbar spine. J Orthop Res 11(2):228–239
25. Stokes I, Mente P, Iatridis J, Farnum C, Aronsson D (2002) Enlargement of growth plate chondrocytes modulated by sustained mechanical loading. J Bone Joint Surg Am 84-A(10):1842–1848
26. Stokes IA, Aronsson DD, Spence H, Iatridis JC (1998) Mechanical modulation of intervertebral disc thickness in growing rat tails. J Spinal Disord 11(3):261–265
27. Taylor TK, Ghosh P, Braund KG, Sutherland JM, Sherwood AA (1976) The effect of spinal fusion on intervertebral disc composition: an experimental study. J Surg Res 21(2):91–104

28. Urban J, Smith S, Fairbank J (2004) Nutrition of the intervertebral disc. Spine 29(23):2700–2709
29. Urban MR, Fairbank JC, Bibby SR, Urban JP (2001) Intervertebral disc composition in neuromuscular scoliosis: changes in cell density and glycosaminoglycan concentration at the curve apex. Spine 26(6):610–617
30. Urban MR, Fairbank JC, Etherington PJ, Loh FL, Winlove CP, Urban JP (2001) Electrochemical measurement of transport into scoliotic intervertebral discs in vivo using nitrous oxide as a tracer. Spine 26(8):984–990
31. Violas P, Estivalezes E, Briot J, Sales de Gauzy J, Swider P (2007) Quantification of intervertebral disc volume properties below spine fusion, using magnetic resonance imaging, in adolescent idiopathic scoliosis surgery. Spine 32(15):E405–E412
32. Yu J, Fairbank J, Roberts S, Urban J (2005) The elastic fiber network of the anulus fibrosus of the normal and scoliotic human intervertebral disc. Spine 30(16):1815–1820